AD_____

AWARD NUMBER: W81XWH-14-1-0242

TITLE: In Vivo Photoacoustic Imaging of Prostate Cancer Using Targeted Contrast Agent

PRINCIPAL INVESTIGATOR: Vikram S Dogra

RECIPIENT: University of Rochester
Rochester, NY 14611

REPORT DATE: November 2016

TYPE OF REPORT: Final

PREPARED FOR: U.S. Army Medical Research and Materiel Command
Fort Detrick, Maryland 21702-5012

DISTRIBUTION STATEMENT: Approved for Public Release;
Distribution Unlimited

REPORT DOCUMENTATION PAGE

Form Approved
OMB No. 0704-0188

1. REPORT DATE	2. REPORT TYPE	3. DATES COVERED
November 2016	Final Report	25 Aug 2014 - 24 Aug 2016

4. TITLE AND SUBTITLE
In vivo Photoacoustic Imaging of Prostate Cancer Using Targeted Contrast Agent

5a. CONTRACT NUMBER
W81XWH-14-1-0242

5b. GRANT NUMBER

5c. PROGRAM ELEMENT NUMBER

6. AUTHOR(S)
Bhargava K Chinni, Shalini Singh, Kent Nastiuk, Hans Schmitthenner, Navalgund Rao
John Krolewski, Vikram Dogra

E-Mail: Vikram_Dogra@urmc.rochester.edu

5d. PROJECT NUMBER

5e. TASK NUMBER

5f. WORK UNIT NUMBER

7. PERFORMING ORGANIZATION NAME(S) AND ADDRESS(ES)

University of Rochester
Rochester, NY - 14642

8. PERFORMING ORGANIZATION REPORT NUMBER

9. SPONSORING / MONITORING AGENCY NAME(S) AND ADDRESS(ES)

U.S. Army Medical Research and Materiel Command
Fort Detrick, Maryland 21702-5012

10. SPONSOR/MONITOR'S ACRONYM(S)

11. SPONSOR/MONITOR'S REPORT NUMBER(S)

12. DISTRIBUTION / AVAILABILITY STATEMENT

Approved for Public Release; Distribution Unlimited

13. SUPPLEMENTARY NOTES

14. ABSTRACT: Prostate specific antigen screening for prostate cancer is inexpensive, non-invasive and sensitive, but lacks specificity. The accuracy of confirmatory prostate biopsy is only 52% due to either the absence of tumor or the inability to precisely sample small tumors with the biopsy needles. Thus, there is an urgent need to develop methods to accurately image cancers within the prostate, to rule out cancer in men with false positive PSA elevation and to ensure successful biopsy for those with small cancers. Photoacoustic imaging is an emerging functional imaging technique that can detect and diagnose prostate cancer based on the near-infrared optical absorption of either endogenous tissue constituents or exogenous contrast agents. Although endogenous tissue constituents show promise, in order to implement photoacoustic imaging in the clinic, there is a need for increased tumor cell specificity, sensitivity and depth of imaging. To enhance the application of photoacoustic imaging for the detection of early stage prostate cancer, development of near infrared dyes - labeled RNA aptamer that recognizes the prostate specific cell surface protein - prostate specific membrane antigen is proposed to specifically image prostate-cancer. The design incorporates a high energy tunable laser as the source and an ultrasound linear array to detect the acoustic-lens-focused photoacoustic signals generated from the cancerous lesions within the prostate.

15. SUBJECT TERMS
Photoacoustic Imaging, Prostate cancer, Near-infrared, targeted molecular imaging agents

16. SECURITY CLASSIFICATION OF:			17. LIMITATION OF ABSTRACT	18. NUMBER OF PAGES	19a. NAME OF RESPONSIBLE PERSON
a. REPORT	b. ABSTRACT	c. THIS PAGE			USAMRMC
Unclassified	Unclassified	Unclassified	Unclassified	24	19b. TELEPHONE NUMBER *(include area code)*

Table of Contents

Page

1. **Introduction…….4**
2. **Keywords…….5**
3. **Accomplishments……...……...6**
4. **Impact……...……13**
5. **Changes/Problems...…..……14**
6. **Products…….…….…….……14**
7. **Participants & Other Collaborating Organizations……15**
8. **Special Reporting Requirements……17**
9. **Appendices……17**

1.INTRODUCTION:

The clinical management of early stage, organ-confined prostate cancer (PrCa) is challenging. The introduction of serum PSA screening in the 1980s lead to a spike in the apparent incidence of PrCa, due to the detection of previously under-diagnosed indolent cancers, which grow slowly and do not affect lifespan[1]. While PSA screening has declined from its peak, most PrCa is still screen-detected and therefore likely to be indolent, requiring no treatment. Unfortunately, there is no reliable technology to identify the rare aggressive cancers among the mass of indolent screen-detected PrCa, which has lead to frequent over-treatment by surgery or radiation. Much effort has focused on the development of tissue or serum biomarkers to differentiate indolent and aggressive disease, but this has not yet yielded sensitive and specific tools. Consequently, the current clinical paradigm for screen-detected PrCa is active surveillance[2, 3] (AS): monitoring by serum PSA testing and serial prostate biopsies to determine the grade (Gleason score) and extent of tumor.

There is an urgent need for imaging tools for AS, i) to confirm the initial PSA-based diagnosis; ii) to guide biopsies, which are now performed in a blinded manner; and iii) to monitor tumor volume, which is currently not measureable but may represent a biomarker of progression from indolent to aggressive disease. Multi-parametric MRI may fill some of these roles, but it is expensive and technically limited[4, 5]. In contrast, photoacoustic imaging (PAI), is an emerging, noninvasive, functional molecular imaging modality that has not yet entered the clinic, and is likely to be less expensive and more portable than any MRI system. The photoacoustic (PA) signal is an ultrasound wave generated by tissue constituents (hemoglobin (Hb), fat, water, etc.) that absorb short (nanosecond) pulses of laser light in the near infra-red (NIR) spectrum[6]. PAI can discriminate among such tissue constituents on the basis of optical absorption properties, allowing for PAI spectroscopy, which can detect biological function[7]. Human PrCa is a viable candidate for PAI since transrectal probes can image the prostate gland *in situ*. Based on ultrasound data from human PrCa patients, we estimate that the distance from the rectal wall to the anterior prostate is ~3.5 cm, which is within the potential range of depth detection for PAI[8]. The most common application of PAI spectroscopy in cancer imaging uses the differences in the absorption spectra of Hb and $Hb0_2$ and is therefore capable of detecting tumors based on regions of hypoxia which promote neo-angiogenesis and more aggressive cancers[9]. However, endogenous tissue constituents such as Hb generate relatively weak photoacoustic signals (due to a small absorptivity factor or extinction coefficient) and lack cancer specificity. Exogenous agents, such as NIR-absorbing dyes linked to tumor-specific binding molecules (such as antibodies) can act as targeted molecular imaging agents (TMIAs) to facilitate sensitive and specific detection of the corresponding cancer. For targeting purposes, prostate surface membrane antigen (PSMA) is detected on the surface of nearly every human PrCa, while expression is low to moderate on non-cancer prostate tissue and very low outside the prostate, making it an excellent biomarker for molecular imaging of PrCa[10]. The initial clinical application of PSMA (ProstaScint) was of limited value because it employed a monoclonal antibody against the cytoplasmic domain of PSMA, detecting only necrotic cells[11]. Subsequently, improved PSMA binding agents have been developed, including a nuclease-stable RNA aptamer (A10-3.2) that binds very efficiently[12]. The PSMA also has an unusual extracellular active site encoding glutamate carboxypeptidase activity, allowing for the synthesis of a peptidomimetic inhibitor (YC-27) that has been linked to a NIR dye for successful *in vivo* imaging of PSMA+ mouse xenografts[13]. Two significant innovations are proposed to enhance

the application of PAI for the detection of early stage PrCa: 1. Use of a NIR dye labeled RNA aptamer that recognizes the prostate specific cell surface protein PSMA to specifically image PrCa and 2. Optimization of multispectral PAI to differentiate small volume, early stage PrCa tumors from surrounding normal prostate tissue.

2.KEYWORDS:

Prostate Cancer
Photoacoustic Imaging
Prostate specific membrane antigen
Targeted Molecular Imaging Agent
Endogenous
Deoxyhemoglobin
Oxyhemoglobin
Near-infrared
C-scan imaging
Acoustic lens
Laser
Ultrasound
Early stage tumors
Exogenous
Contrast agents
Cancer cell lines
Cancer detection

3. ACCOMPLISHMENTS:

What were the major goals of the project?

1. Identify and synthesis of the near-infrared dyes and perform photoacoustic experiments in-vitro.
2. Conjugation of the tested near-infrared dyes with prostate cancer cell lines and perform photoacoustic imaging experiments.
3. Determination of the sensitivity of the acoustic lens based photoacoustic imaging system in classifying the positive prostate cancer cells from negative prostate cancer cells.

What was accomplished under these goals?

- Identification of IRDye800CW as an exogenous contrast agent for PAI.
- Demonstration of increased sensitivity of IRDye800CW versus other labels using our acoustic lens based PAI device.
- PAI discrimination of PrCa cells expressing PSMA (C4-2) versus non-expressing prostate cancer cells (PC3) using IRDye800 conjugated with A10.3 aptamer bonded to PSMA.
- PAI discrimination of PrCa cells expressing PSMA (C4-2) versus non-expressing prostate cancer cells (PC3) using IRDye800 conjugated with YC-27, a peptidomimetic urea inhibitor bonded to PSMA.

PROJECT SUMMARY:

Limitations of endogenous contrast agents for prostate cancer diagnosis. While pre-clinical testing of prostate resection slices indicates that Photoacoustic Imaging (PAI) has higher sensitivity and specificity than TRUS, imaging depth is limited, andchromophores such as de-oxyhemoglobin (dHb) and oxyhemoglobin (HbO_2) have two limitations: i) their small absorptivity factor (extinction coefficient) leads to weak PA signals, limiting the depth of tumor detection as well as the minimal detectable tumor size; and ii) endogenous molecules have little specificity for cancer. In order to improve depth penetration and image quality, exogenous chromophores can be

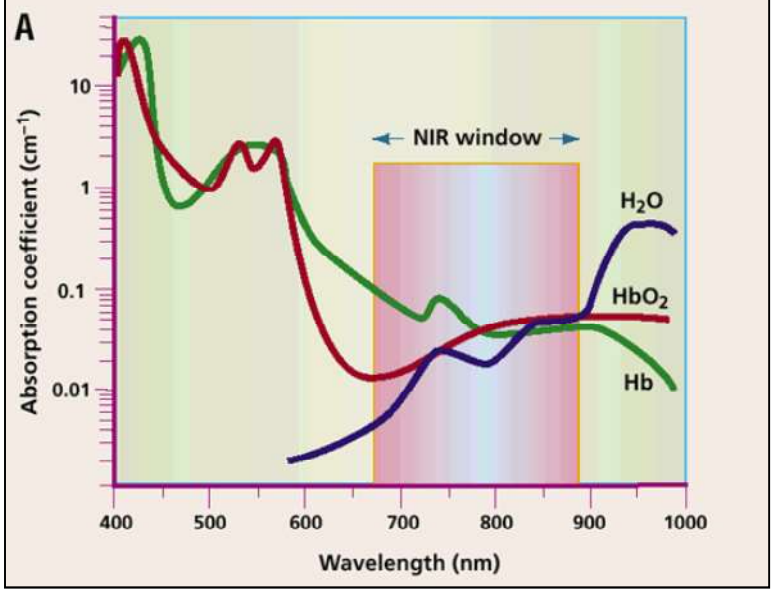

Fig. 1. Biological imaging near-infrared window.

employed to enhance sensitivity relative to endogenous agents. This approach has been demonstrated in the use of a near infrared fluorescent (NIRF) dye, IR800CW conjugated to a peptide that targets the neutropilin-1 receptor for the PAI of breast cancer. Excitation of cells can be optimized by use of a laser tuned to the maximum wavelength of NIR dyes with absorptivity factors two to three orders of magnitude greater than those of endogenous agents. Unlike fluorescence imaging with light as the input and backscattered radiation as the output, PA imaging uses light as the input source for excitation but detection and image formation use ultrasound waves generated by the tissue. Since ultrasonic waves scatter much less than light in the tissue, PAI can produce higher resolution imaging deep in tissue, compared to fluorescent detection. For greater tissue depth penetration and sensitivity, PAI utilizes dyes that absorb in the 'biological NIR window' between 700-900 nm. The optimal NIR window is designed to circumvent the strong absorbance of Hb, HbO_2 and H_2O as shown in Fig. 1. NIR dyes related to ICG including Cy7, Alexa750 and IR800CW are ideal and offer a dramatic increase in sensitivity.

Identification of IRDye800CW as an exogenous contrast agent for PAI. To quantify the PA signal generated with tunable laser excitation in the 700-1000 nm range of endogenous or exogenous dye components, algorithms have been developed to de-convolute the individual chromophore PA images. Five dyes (IRDye800CW, AlexaFluor750, Cy7-NHS-ester, Cy7-sulfo and Dylight800) were tested using our acoustic lens based device at 100 micromolar (μM) concentration. A water bath setup (Fig. 2) was used to determine the photoacoustic spectra of these five dyes. Each contrast agent was interrogated in the NIR region in a five step-interval range and PA signals recorded using our PAI probe. These recorded PA signals were further processed to find the absorption maxima for each exogenous contrast agent across the NIR region. The PA absorption spectra of each dye have been plotted as shown in the Fig. 3. As expected from the reported peak intensities (lambda max) in the ultraviolet-visible spectra, the Alexafluor 750 has a peak PA signal when irradiated at 750 nm, Cy7-NHS-ester at 760 nm, Cy7-sulfo at 755 nm, Dylight800 at 785 nm and the dye IR800CW has a peak signal at 775 nm. When the targeted molecular imaging agents (TMIAs) are injected into the blood stream and PA imaging is conducted during wash out period, the

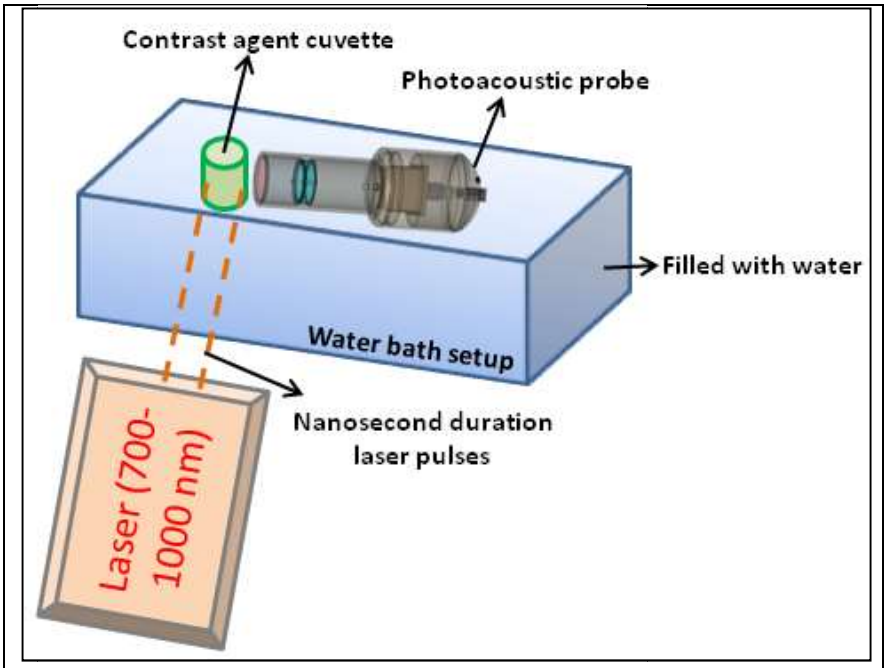

Fig. 2. Spectral analysis of near-infrared dyes. Contrast agents in a cuvette have been examined for a photoacoustic signal using the laser from 700 nm to 1000 nm wavelength.

image signal will be the linear sum of signal from all the underlying dominant chromophores (dHb, HbO_2 and NIR dye). It is important to create separate images of individual chromophores to obtain the signature related to only the specific biomarker. This task requires input data from the PA signal spectrum of endogenous or exogenous dye components and algorithms have been developed to de-convolve the individual chromophore images to determine i) their sensitivity by comparing their PA yield (PA signal per micro molar solution), and ii) their spectra shape. Among the five contrast agents/dyes we investigated, IRDye800CW was chosen based on photoacoustic spectrum analysis as determined by the highest intensity achieved relative to the other agents and because the peak absorption is well separated from endogenous tissue constituents, as shown in Figure 3. The initial aim of the project was to use CY7 as the photoacoustic contrast dye. When we started testing, however, we obtained weak photoacoustic intensity with CY7 and needed to search for an alternative dye for a stronger photoacoustic signal[14]. We therefore tested five dyes by both visible absorption spectra and photoacoustic spectroscopy. The un-normalized spectra of the tested five dyes are shown in Fig. 4. The dye showing superior absorption at equimolar concentrations after exposure to room light for three hours was IR800CW followed by Alexa 750 with considerable less absorption by Cy7, sulfo-Cy7 and Dylite. In subsequent results, IR800CW also displayed the best solution stability. Consistent with this data, the IRDye800CW showed better sensitivity and higher photoacoustic signal versus CY7 (Fig. 3). As a result, IRDye800CW was chosen as a replacement for CY7 in subsequent studies as it was shown to provide optimal signal contrast and better stability in handling and the laser compared to the CY7. In addition, IRDye800CW displays distinctive photoacoustic peak absorption at 775 nm which enables better differentiation from endogenous chromophores.

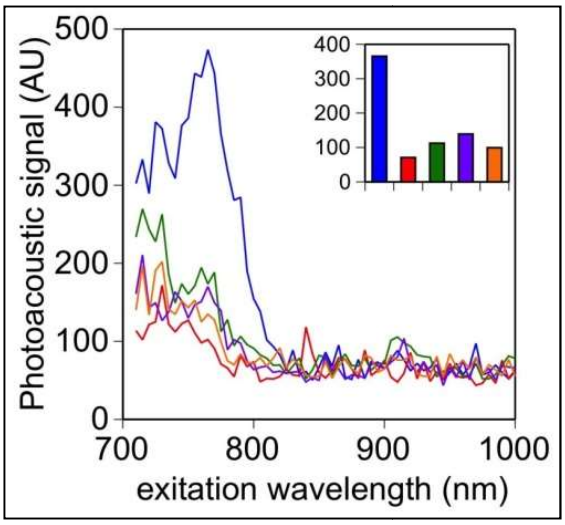

Fig. 3. PA spectra of five contrast agents. IRdye800CW (blue); AlexaFluor750 (red); Cy7-NHS-ester (green); Cy7-sulfo (orange); Dylight800 (purple).

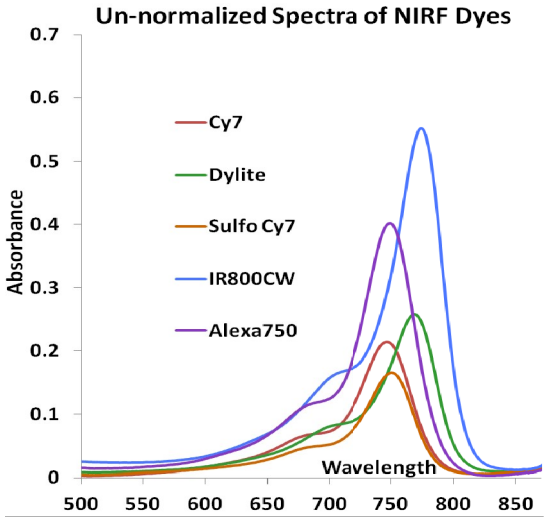

Fig. 4. Optical absorption spectra of five contrast agents. IRdye800CW (blue); AlexaFluor750 (purple); Cy7-NHS-ester (red); Cy7-sulfo (orange); Dylight800 (green).

Sensitivity of IRDye800CW using our PAI device. The IRDye800CW was diluted from 50 µM to 90 nM concentrations and photoacoustic signal measured to obtain the sensitivity of the IRDye800CW. Each red square in the plot represents the corresponding IRDye800CW concentration on the x axis and its PA signal intensity on the y axis. PA signal from the dimethyl sulphoxide and de-ionized water has been subtracted from each recorded value and PA signal from the dye alone has been plotted. Using our current PAI system, 90 nanomolar (nM) was determined to be the threshold for signal above noise (Fig. 5).

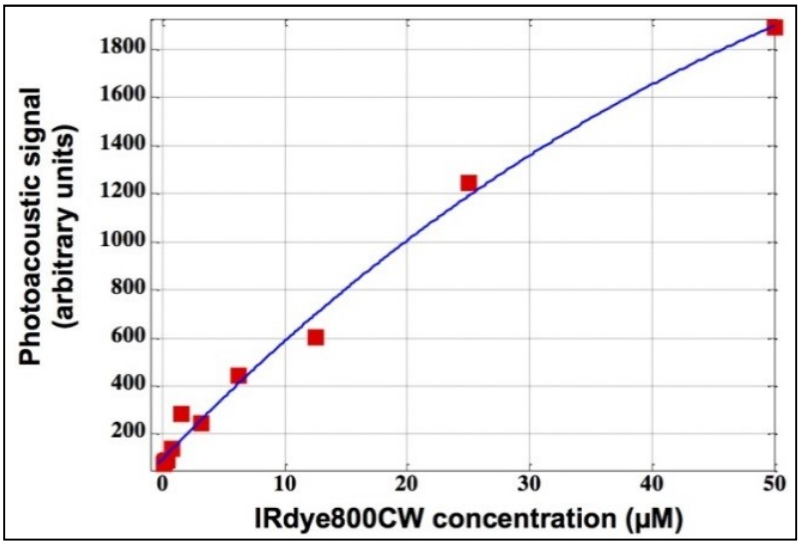

Fig. 5. Sensitivity of IRDye800CW using our PAI device. IRDye800 concentration varied from 90 nM to 50 µM. Each red square represents the corresponding IRDye800CW concentration and its PA signal intensity.

PAI of PrCa cells using IRDye800 conjugated with TMIA bonded to PSMA. Among the five contrast agents/dyes we investigated, IRDye800CW was chosen because it produced the highest PA intensity relative to the other agents and because the peak absorption is well separated from endogenous tissue constituents (Fig. 3). IRdye800CW was serially diluted in DMSO and water. The resultant PA signal intensity above diluent signal correlates well with concentration (r^2 = 0.979, Fig. 5). Using our PAI apparatus, 0.8 µM IRDye800CW is the threshold for detecting signal above noise of the NIR dyes tested.

A TMIA was synthesized by labeling the PSMA specific 10.3.2 aptamer with IRDye800CW (GeneLink). Cells expressing (C4-2) or lacking (PC3) PSMA were incubated in a 4 µM solution of the TMIA in PBS, washed thrice in PBS by centrifugation and resuspension, and

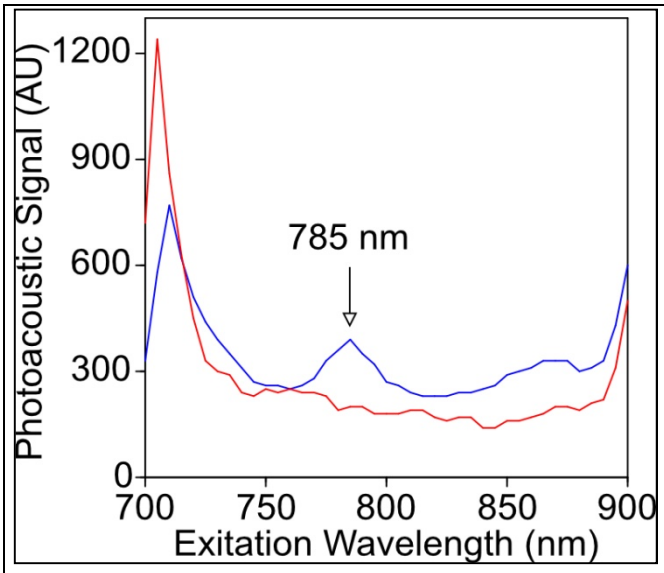

Fig. 6. Specific labeling by TMIA for PAI. PSMA- PC3 (red) and PSMA+ C4-2 (blue) prostate cancer cells were labeled with A10-3.2-IRDye800CW and scanned from 700 nm to 900 nm wavelength laser light in the setup depicted in Fig. 2.

examined in our PAI system. The spectra of the photoacoustic signal from C4-2 cells and PC3 cells shows a peak of maximal PA signal difference at 785 nm. The 20 nm difference between the peak absorbance of the IRdye800CW at 765 nm and this 785 nm peak suggests that conjugation of the IRDye800CW to the aptamer to constitute the TMIA, and/or binding of TMIA to the PSMA molecules on the prostate cell surface, affected the wavelength of absorbance producing peak PA signal (Fig. 6).

Quantitative characterization of this TMIA shows specific and uniform binding to PSMA expressing prostate cancer cells. Four samples of ten million PC3 or C4-2 cells were labeled as above and optically imaged at 770 nm (Fig. 7a) and quantitated (Fig. 7b) using an IVIS spectrum (PerkinElmer). TMIA labeling was uniform (CV = 5.5% for PC3, 6.0% for C4-2), and the signal (C4-2) to noise (PC3) ratio (SNR) was 2.56 +/- 0.08. One of the four samples of these TMIA labeled cell samples was used to tune the PA system alignment, and the remaining three were pipetted into cuvettes and peak PA signal determined at 785 nm excitation from a B-scan (Fig. 7c) and when quantitated the SNR was 2.33 +/- 0.09 (Fig. 7d). The data is reconstructed as C-scan for each cuvette of C4-2 cells (Fig. 7e) and PC3 cells (Fig. 7f). Analyzing the C-scans using an ROI encompassing the cuvette, the SNR was 5.35 +/- 0.04.

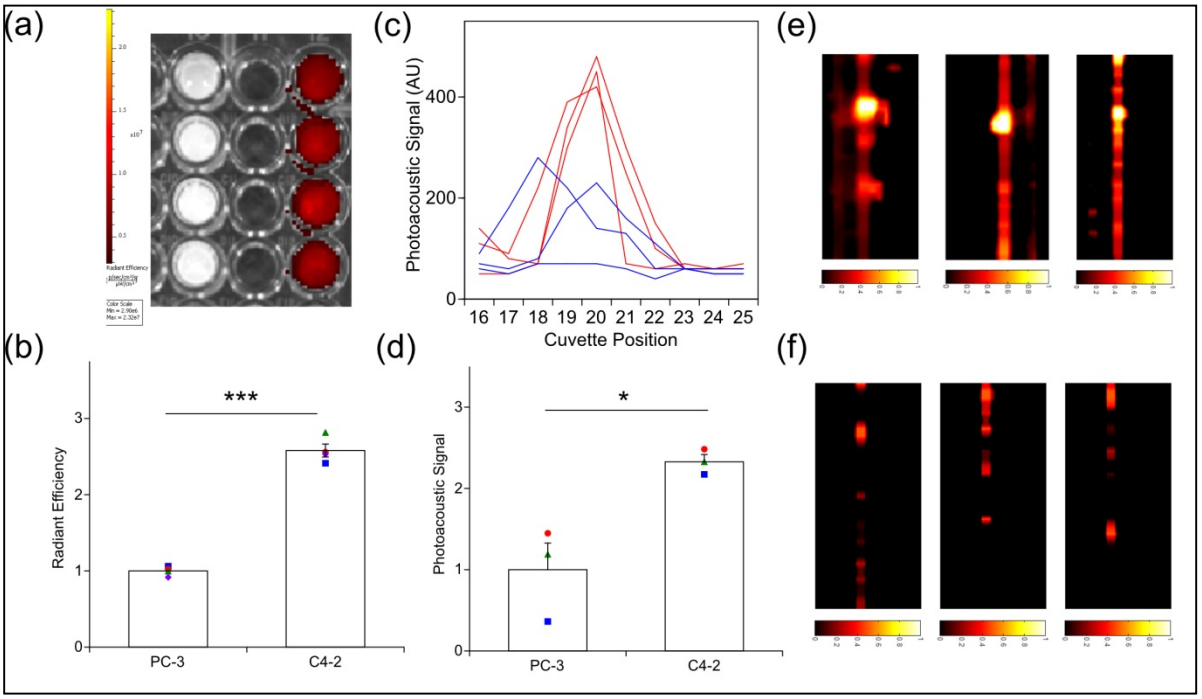

Fig. 7 Enhanced photoacoustic signal from PSMA+ C4-2 prostate cancer cells labeled with A10-3.2-IRdye800CW aptamer-dye. Optical imaging of a twelve well plate containing aliquots of PSMA+ C4-2 (right side 4 wells) and PSMA- PC3 (left side 4 wells) cells labeled with aptamer-dye, (or buffer in middle wells). Fluorescent signal intensity was captured via IVIS (a) and relative intensity plotted (b). The cells were sequentially loaded into the PAI instrument cuvette (Fig 2) and PA signal was captured at 785 nm, by scanning along the long axis of the cuvette (B-scan) (c) and peak PA signal was plotted, p = 0.0174 (d). C-scan images of cuvettes containing C4-2 (e) and PC3 (f).

An alternate targeting moiety, YC-27, comprising a peptidomimetic urea inhibitor, DCL, conjugated to IRDye800CW (Licor), was similarly evaluated. The 20 nm shift in the wavelength of absorbance producing peak PA signal was also apparent (DNS). The YC-27 TMIA also shows specific and uniform binding to PSMA expressing prostate cancer cells as assessed by optically imaging at 770 nm (Fig. 8a and 8b). YC-27 TMIA labeling was higher than for the aptamer TMIA (CV = 17% for PC3, 9.9% for C4-2), but the SNR was much greater, 24.7 +/- 1.22, minimizing the impact of the slight increase in labeling variability. Peak PA signal was determined from a B-scan for each cell type after labeling with the YC-27 TMIA (Fig. 8c) and when quantitated the SNR was 1.86 +/- 0.24 (Fig. 8d). The data is reconstructed as C-scan for each cuvette of C4-2 cells (Fig. 8e) and PC3 cells (Fig. 8f). Analyzing the C-scans using an ROI encompassing the cuvette, the SNR was 5.91 +/- 0.81.

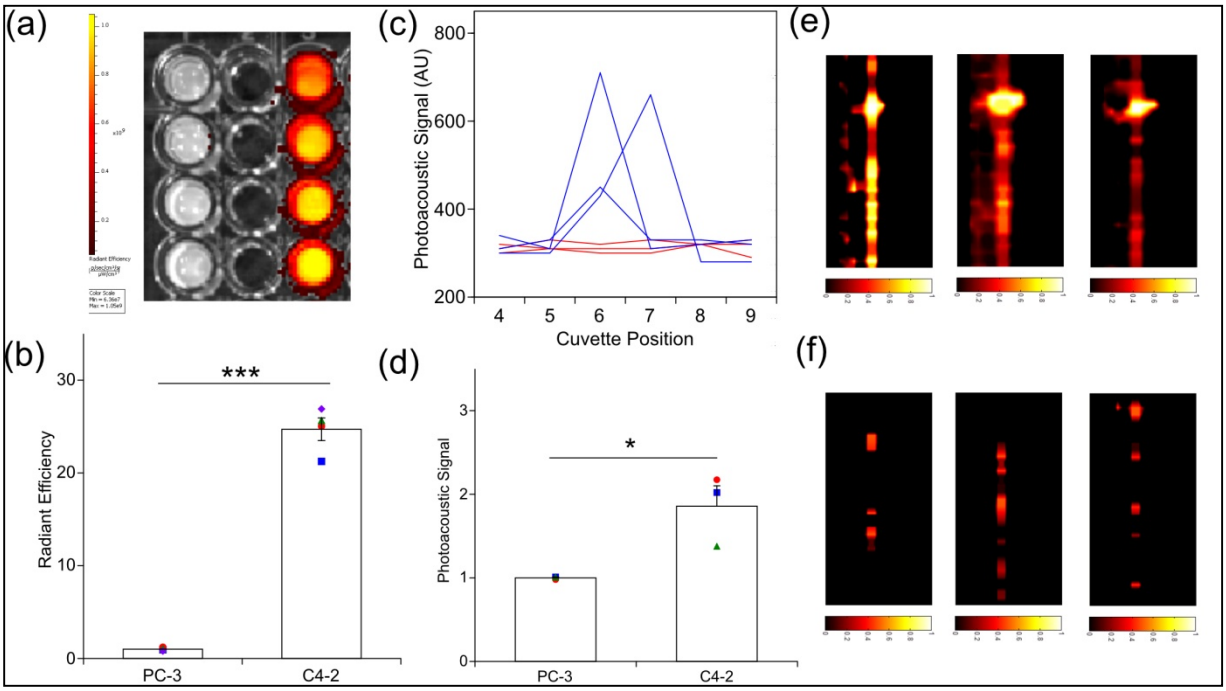

Fig. 8 Enhanced photoacoustic signal from PSMA+ C4-2 prostate cancer cells labeled with YC27-IRdye800CW urea-dye. Optical imaging of a twelve well plate containing aliquots of PSMA+ C4-2 (right side 4 wells) and PSMA- PC3 (left side 4 wells) cells labeled with urea-dye, (or buffer in middle wells). Fluorescent signal intensity was captured via IVIS (a) and relative intensity plotted (b). The cells were sequentially loaded into the PAI instrument cuvette (Fig 2) and PA signal was captured at 785 nm, by scanning along the long axis of the cuvette (B-scan) (c) and peak PA signal was plotted, p = 0.0246 (d). C-scan images of cuvettes containing C4-2 (e) and PC3 (f) are shown.

CONCLUSION: TMIAs optimized for PAI, in combination with an acoustic lens, allowed us to discriminate between prostate cancer cells lines that either express PSMA or do not express PSMA. Both the A10 aptamer and the PSMA inhibitor in YC-27 specifically bind PSMA-expressing cells and can be successfully delivered *in vivo,* i.p. or intra-tumorally[12, 15-17]. While the aptamer TMIA showed good SNR for PAI, it is expensive to synthesize and less stable than the inhibitor. Conjugation of modified

chromophores to the inhibitor DCL is more tractable [17] and thus represents an immediately available approach for use in developing "louder" targeted agents to detect PrCa by PAI.

With successful completion of this research, we will have a device and an accompanying molecular imaging reagent that can be readily moved into human clinical trials. We believe that this work will ultimately yield a real-time, safe and effective imaging device that has a potential to aid in the diagnosis of early stage prostate cancer and reduce patient anxiety (due to the need for biopsy and repeat biopsy) and also reduce the amount of over-treatment of prostate cancer.

REFERENCES:

1. R. L. Siegel, K. D. Miller, and A. Jemal, "Cancer statistics, 2016" CA Cancer J Clin 66, 7-30 (2016). doi:10.3322/caac.21332
2. M. L. McDonald, and J. K. Parsons, "The Case for Tailored Prostate Cancer Screening: An NCCN Perspective" J Natl Compr Canc Netw 13, 1576-1583 (2015).
3. S. M. Bruinsma et al., "Active surveillance for prostate cancer: a narrative review of clinical guidelines" Nat Rev Urol 13, 151-167 (2016). doi:10.1038/nrurol.2015.313
4. D. Fehr et al., "Automatic classification of prostate cancer Gleason scores from multiparametric magnetic resonance images" Proc Natl Acad Sci U S A 112, E6265-6273 (2015). doi:10.1073/pnas.1505935112
5. S. S. Salami et al., "Multiparametric magnetic resonance imaging outperforms the Prostate Cancer Prevention Trial risk calculator in predicting clinically significant prostate cancer" Cancer 120, 2876-2882 (2014). doi:10.1002/cncr.28790
6. K. S. Valluru, B. K. Chinni, and N. A. Rao, "Photoacoustic imaging: opening new frontiers in medical imaging" J Clin Imaging Sci 1, 24 (2011). doi:10.4103/2156-7514.80522
7. S. Mallidi, G. P. Luke, and S. Emelianov, "Photoacoustic imaging in cancer detection, diagnosis, and treatment guidance" Trends Biotechnol 29, 213-221 (2011). doi:10.1016/j.tibtech.2011.01.006
8. S. Zackrisson, S. M. van de Ven, and S. S. Gambhir, "Light in and sound out: emerging translational strategies for photoacoustic imaging" Cancer Res 74, 979-1004 (2014). doi:10.1158/0008-5472.CAN-13-2387
9. M. Mehrmohammadi et al., "Photoacoustic Imaging for Cancer Detection and Staging" Curr Mol Imaging 2, 89-105 (2013). doi:10.2174/2211555211302010010
10. P. Mhawech-Fauceglia et al., "Prostate-specific membrane antigen (PSMA) protein expression in normal and neoplastic tissues and its sensitivity and specificity in prostate adenocarcinoma: an immunohistochemical study using mutiple tumour tissue microarray technique" Histopathology 50, 472-483 (2007). doi:10.1111/j.1365-2559.2007.02635.x
11. P. M. Smith-Jones et al., "In vitro characterization of radiolabeled monoclonal antibodies specific for the extracellular domain of prostate-specific membrane antigen" Cancer Res 60, 5237-5243 (2000).
12. J. P. Dassie et al., "Systemic administration of optimized aptamer-siRNA chimeras promotes regression of PSMA-expressing tumors" Nat Biotechnol 27, 839-849 (2009). doi:10.1038/nbt.1560

13. Y. Chen et al., "A low molecular weight PSMA-based fluorescent imaging agent for cancer" Biochem Biophys Res Commun 390, 624-629 (2009). doi:10.1016/j.bbrc.2009.10.017
14. Berlier JE, Rothe A, Buller G, Bradford J, Gray DR, Filanoski BJ, Telford WG, Yue S, Liu J, Cheung CY, Chang W, Hirsch JD, Beechem JM, Haugland RP, Haugland RP. (2003) Quantitative comparison of long-wavelength Alexa Fluor dyes to Cy dyes: fluorescence of the dyes and their bioconjugates. J Histochem Cytochem; 51(12):1699-712. PMID: 14623938
15. J. O. McNamara, 2nd et al., "Cell type-specific delivery of siRNAs with aptamer-siRNA chimeras" Nat Biotechnol 24, 1005-1015 (2006). doi:10.1038/nbt1223
16. X. Ni et al., "Prostate-targeted radiosensitization via aptamer-shRNA chimeras in human tumor xenografts" J Clin Invest 121, 2383-2390 (2011). doi:10.1172/JCI45109
17. Y. Chen et al., "Synthesis and biological evaluation of low molecular weight fluorescent imaging agents for the prostate-specific membrane antigen" Bioconjug Chem 23, 2377-2385 (2012). doi:10.1021/bc3003919

What opportunities for training and professional development has the project provided?
Nothing to Report.

How were the results disseminated to communities of interest?
Journal publications and presentations at scientific conferences.

What do you plan to do during the next reporting period to accomplish the goals?
Nothing to Report.

4. Impact:

What was the impact on the development of the principal discipline(s) of the project?
The use of photoacoustic imaging (PAI) technology in conjunction with two molecular imaging agents that specifically target the prostate-specific membrane antigen (PSMA) expressed on the tumor cell surface of most prostate cancers. We demonstrated successful imaging of phantoms containing cancer cells labeled with either of two different PSMA-targeting agents, the ribonucleic acid aptamer A10-3.2 and a urea-based peptidomimetic inhibitor, each linked to the near-infrared dye IRDye800CW. By specifically targeting cells with these agents linked to a dye chosen for optimal signal, we are able to discriminate prostate cancer cells that express PSMA.

Major accomplishments and innovations:

- Identification of IRDye800CW as an exogenous contrast agent for PAI.
- Demonstration of increased sensitivity of IRDye800CW versus other labels using our acoustic lens based PAI device.
- PAI discrimination of PrCa cells expressing PSMA (C4-2) versus non-expressing prostate cancer cells (PC3) using IRDye800 conjugated with A10.3 aptamer bonded to PSMA.

- PAI discrimination of PrCa cells expressing PSMA (C4-2) versus non-expressing prostate cancer cells (PC3) using IRDye800 conjugated with YC-27, a peptidomimetic urea inhibitor bonded to PSMA.

What was the impact on other disciplines? Nothing to Report.
What was the impact on technology transfer? Nothing to Report.
What was the impact on society beyond science and technology? Nothing to Report.

5. **Changes/Problems:**
Changes in approach and reasons for change. Nothing to Report.

Actual or anticipated problems or delays and actions or plans to resolve them. Nothing to Report.

Changes that had a significant impact on expenditures: Nothing to Report.

Significant changes in use or care of human subjects, vertebrate animals, biohazards, and/or select agents. Nothing to Report.

6. **Products:**

Publications, conference papers, and presentations

Journal publication

Dogra V, Chinni B, Singh S, Schmitthenner H, Rao N, Krolewski JJ, Nastiuk KL. (2016) **Photoacoustic imaging with an acoustic lens detects prostate cancer cells labeled with PSMA-targeting near-infrared dye-conjugates**. J Biomed Opt; 21(6):66019. *published; acknowledgement of federal support (yes).*

Books or other non-periodical, one-time publications: None

Presentations:
Quantitative volume determination of normal, neoplastic and hyperplastic mouse prostate using ultrasound imaging (2014) Shalini Singh*, Chunliu Pan*, Ronald Wood[¶,§], Guang-Qian Xiao*, Chiuan-Ren Yeh[§], Shuyuan Yeh[§], Kai Sha*, John J. Krolewski*, Kent L. Nastiuk*. James P Wilmot cancer institute 19th annual scientific symposium. University of Rochester, NY.

Bhargava K Chinni, Shalini Singh, Kent Nastiuk, Hans Schmitthenner, Navalgund Rao, John Krolewski, Vikram Dogra. (2014) **Detecting the sound of light to classify cancer from benign**. James P Wilmot cancer institute 19th annual scientific symposium. University of Rochester, NY.

Lauren Heese, Hans Schmitthenner, Nnamdi Akporji, Michael Regan, Bhargava Chinni, Navalgund Rao, Vikram Dogra. (2015) **Modular Synthesis of Targeted Near Infrared**

Agents for Photoacoustic Imaging of Cancer. World Molecular Imaging Congress, September 2-5, Honolulu, Hawaii.

Hans Schmitthenner, Bhargava Chinni, Shalini Singh, Lauren Heese, Ryan Le Tourneau, A. Karim Ebong, Irene M. Evans, Kent L. Nastiuk, John Krolewski, Navalgund Rao, Vikram Dogra. (2016) **PSMA-targeted Near Infrared Dye Imaging Agents for Photoacoustic Imaging of Prostate Cancer**. Accepted for oral presentation in World Molecular Imaging Congress, September 7-10, 2016, New York.

Website(s) or other Internet site(s): None

Technologies or techniques: None

Inventions, patent applications, and/or licenses: None

Other Products:

- Identification of IRDye800CW as an exogenous contrast agent for photoacoustic imaging (PAI).
- Demonstration of increased sensitivity of IRDye800CW versus other labels using our acoustic lens based PAI device.
- PAI discrimination of PrCa cells expressing prostate-specific membrane antigen (C4-2) versus non-expressing prostate cancer cells (PC3) using IRDye800 conjugated with A10.3 aptamer bonded to prostate-specific membrane antigen (PSMA).
- PAI discrimination of PrCa cells expressing PSMA (C4-2) versus non-expressing prostate cancer cells (PC3) using IRDye800 conjugated with YC-27, a peptidomimetic urea inhibitor bonded to PSMA.

7. PARTICIPANTS & OTHER COLLABORATING ORGANIZATIONS.

What individuals have worked on the project?

Name: Vikram Dogra, M.D.

Role: Principal Investigator

Nearest person month worked: 1

Contribution to Project: Dr. Dogra is Professor of Radiology, Urology and Biomedical Engineering at University of Rochester. He has over 30 years of experience in diagnostic and clinical research with several imaging modalities such as Ultrasound, Magnetic resonance imaging and Computed tomography. His research laboratory at University of Rochester primarily focuses on Photoacoustic imaging. His special skills include organizational capacity, leadership, and in-depth clinical knowledge in applications of ultrasound and problems faced in the detection of cancer. He directly oversaw all of the work performed in the project and guided the entire team towards achieving the objectives.

Name: John Krolewski, M.D., Ph.D.

Role: Co-Investigator

Nearest person month worked: 1

Contribution to Project: Dr. Krolewski is a Professor of Pathology and Laboratory Medicine and has been investigating mechanisms of cell death and cytokine signaling in the prostate for over 20 years. He directed the cell studies involved in this project.

Name: Kent Nastiuk, Ph.D.

Role: Co-Investigator

Nearest person month worked: 2

Contribution to Project: Dr. Nastiuk is an Associate Professor of Pathology and Laboratory Medicine. He has carried out much of the generation of biological models for this project. He has over 15 years of experience investigating signaling in the prostate, and is well versed in both cell culture and animal models for prostate cancer growth.

Name: Bhargava Chinni, MS

Role: Research Associate

Nearest person month worked: 7

Contribution to Project: Bhargava has performed all the photoacoustic experiments in this project and studied the spectrums of the near-infrared contrast agents, imaging, data acquisition, image processing tasks and data analysis under Dr. Rao's supervision. He has worked on Photoacoustic Imaging over 5 years with Dr. Dogra and Dr. Rao. He has performed several in-vitro phtoacoustic experiments in Dr. Dogra's laboratory at University of Rochester.

Name: Navalgund Rao, PhD

Role: Consultant

Nearest person month worked: 1

Contribution to Project: Dr. Rao is a Research Professor at Rochester Institute of Technology in the Center for Imaging Sciences department. He has over 30 years of expertise in the field of ultrasound imaging. Dr. Rao oversaw all the photoacoustic imaging experimental work and image analysis tasks performed in this project.

Name: Hans Schmitthenner, PhD

Role: Consultant

Nearest person month worked: 1

Contribution to Project: Dr. Schmitthenner is a Research Scientist at Rochester Institute of Technology. He oversaw the synthesis of the contrast agents investigated in this project.

Name: Shalini Singh, PhD

Role: Post Doc

Nearest person month worked: 3

Contribution to Project: Dr. Singh has performed all the IVIS experiments in this project at University of Rochester. Dr. Nastiuk and Dr. Krolewski has guided Dr. Singh in performing the conjugation of prostate cancer cell lines with the contrast agents and perform fluorescence experiments using IVIS machine.

Has there been a change in the active other support of the PD/PI(s) or senior/key personnel since the last reporting period? Nothing to Report.

What other organizations were involved as partners? Nothing to Report.

8. SPECIAL REPORTING REQUIREMENTS: None

9. APPENDICES:

Quantitative volume determination of normal, neoplastic and hyperplastic mouse prostate using ultrasound imaging: Genetically engineered mouse models are essential to the investigation of the molecular mechanisms underlying human prostate pathology and the effects of therapy on the diseased prostate. Serial *in vivo* volumetric imaging expands the scope and accuracy of experimental investigations of models of normal prostate physiology, benign prostatic hyperplasia and prostate cancer, which are otherwise limited by the anatomy of the mouse prostate. Moreover, accurate imaging of hyperplastic and tumorigenic prostates is now recognized as essential to rigorous pre-clinical trials of new therapies. Bioluminescent imaging has been widely used to determine prostate tumor size, but is semi-quantitative at best. Magnetic resonance imaging can determine prostate volume very accurately, but is expensive and has low throughput. We therefore sought to develop and implement a high throughput, low cost, and accurate serial imaging protocol for the mouse prostate.

Detecting the sound of light to classify cancer from benign: Prostate specific antigen screening for prostate cancer is inexpensive, non-invasive and sensitive, but lacks specificity. The accuracy of confirmatory prostate biopsy is only 52% due to either the absence of tumor or the inability to precisely sample small tumors with the biopsy needles. Thus, there is an urgent need to develop methods to accurately image cancers within the prostate, to rule out cancer in men with false positive PSA elevation and to ensure successful biopsy for those with small cancers. Photoacoustic imaging is an emerging functional imaging technique that can detect and diagnose prostate cancer based on the near-infrared optical absorption of either endogenous tissue constituents or exogenous contrast agents. Although endogenous tissue constituents show promise, in order to implement photoacoustic imaging in the clinic, there is a need for increased tumor cell specificity, sensitivity and depth of imaging. To enhance the

application of photoacoustic imaging for the detection of early stage prostate cancer, development of near infrared dyes - labeled RNA aptamer that recognizes the prostate specific cell surface protein - prostate specific membrane antigen is proposed to specifically image prostate-cancer. The design incorporates a high energy tunable laser as the source and an ultrasound linear array to detect the acoustic-lens-focused photoacoustic signals generated from the cancerous lesions within the prostate.

Modular Synthesis of Targeted Near Infrared Agents for Photoacoustic Imaging of Cancer: Photoacoustic imaging (PAI) is a sensitive, non-invasive means of detecting cancer and is poised to become a transformative method for early screening, targeted biopsies and monitoring disease progression. A key innovation needed in PAI is the design of 'high-gain" imaging agents which can readily be prepared and conjugated to groups which target biomarkers in diseased cells. The current technology relies on using endogenous dyes such as deoxyhemoglobin or oxy-hemoglobin. The goal is to provide a versatile and broadly applicable synthesis of peptide-based agents combining high-gain NIR dyes that may be conjugated to a PSMA inhibitor for the early detection of prostate cancer by PAI. There is a precedent for the use of a targeted exogenous NIR dye, IR800CW, conjugated to a peptide specific for neutropilin yielding a photoacoustic signal.

PSMA-targeted Near Infrared Dye Imaging Agents for Photoacoustic Imaging of Prostate Cancer: Photoacoustic imaging (PAI) is an emerging noninvasive modality poised to enter the clinic. PAI is well-suited for early, specific detection of prostate cancer (PrCr) and to guide biopsies and active surveillance. In most cases the ultrasound signal in PAI is generated by endogenous chromophores such as hemoglobin energized from nanosecond pulses of a near infra-red (NIR) laser. High absorptivity exogenous agents, such as NIR dyes linked to tumor-specific targeting molecules have been shown to enhance the sensitivity in PAI of breast cancer models. However, reports of exogenous NIR dye based targeted molecular imaging agents (TMIAs) for PAI of PrCa and for other cancers are sparse. To meet this need we envisioned a collaboration which combines a new method of evaluating NIR agents by a novel PAI instrument with a new modular synthesis of TMIAs. For targeting purposes, prostate surface membrane antigen (PSMA) expressed in PrCa cells, and with low expression in non-cancer tissue, is an excellent biomarker for imaging PrCa. Two targeting agents have shown high affinity for PSMA, a nuclease-stable RNA aptamer (A10-3.2) and a urea inhibitor (DCL) which has been coupled with NIR dyes to form TMIAs such as YC-27 and to F agents for PET of PrCa. Our goal was to utilize these motifs and compare binding by fluorescence and PA signal of both the aptamer and the urea targeting systems and to confirm the PSMA binding by confocal fluorescence microscopy.

Journal of Biomedical Optics

BiomedicalOptics.SPIEDigitalLibrary.org

Photoacoustic imaging with an acoustic lens detects prostate cancer cells labeled with PSMA-targeting near-infrared dye-conjugates

Vikram Dogra
Bhargava Chinni
Shalini Singh
Hans Schmitthenner
Navalgund Rao
John J. Krolewski
Kent L. Nastiuk

Vikram Dogra, Bhargava Chinni, Shalini Singh, Hans Schmitthenner, Navalgund Rao, John J. Krolewski, Kent L. Nastiuk, "Photoacoustic imaging with an acoustic lens detects prostate cancer cells labeled with PSMA-targeting near-infrared dye-conjugates," *J. Biomed. Opt.* **21**(6), 066019 (2016), doi: 10.1117/1.JBO.21.6.066019.

Photoacoustic imaging with an acoustic lens detects prostate cancer cells labeled with PSMA-targeting near-infrared dye-conjugates

Vikram Dogra,[a] Bhargava Chinni,[a,†] Shalini Singh,[b,†] Hans Schmitthenner,[c,d] Navalgund Rao,[c] John J. Krolewski,[b,e] and Kent L. Nastiuk[b,*]
[a]University of Rochester, Department of Image Science, 601 Elmwood Avenue, Rochester, New York 14642, United States
[b]Roswell Park Cancer Institute, Department of Cancer Genetics, Elm and Carlton Streets, Buffalo, New York 14263, United States
[c]Rochester Institute of Technology, Carlson Center for Imaging Science, 54 Lomb Memorial Drive, Rochester, New York 14623, United States
[d]Rochester Institute of Technology, School of Chemistry and Materials Science, 54 Lomb Memorial Drive, Rochester, New York 14623, United States
[e]Roswell Park Cancer Institute, Center for Personalized Medicine, Elm and Carlton Streets, Buffalo, New York 14263, United States

Abstract. There is an urgent need for sensitive and specific tools to accurately image early stage, organ-confined human prostate cancers to facilitate active surveillance and reduce unnecessary treatment. Recently, we developed an acoustic lens that enhances the sensitivity of photoacoustic imaging. Here, we report the use of this device in conjunction with two molecular imaging agents that specifically target the prostate-specific membrane antigen (PSMA) expressed on the tumor cell surface of most prostate cancers. We demonstrate successful imaging of phantoms containing cancer cells labeled with either of two different PSMA-targeting agents, the ribonucleic acid aptamer A10-3.2 and a urea-based peptidomimetic inhibitor, each linked to the near-infrared dye IRDye800CW. By specifically targeting cells with these agents linked to a dye chosen for optimal signal, we are able to discriminate prostate cancer cells that express PSMA. [DOI: 10.1117/1.JBO.21.6.066019]

Keywords: photoacoustic imaging; prostate; prostate-specific membrane antigen; near-infrared; aptamer; acoustic lens.

Paper 160162LRR received Mar. 15, 2016; accepted for publication Jun. 13, 2016; published online Jun. 30, 2016.

1 Introduction

The clinical management of early stage, organ-confined prostate cancer (PrCa) is challenging. The introduction of serum prostate-specific antigen (PSA) screening in the 1980s led to a spike in the apparent incidence of PrCa, due to the detection of previously underdiagnosed indolent cancers, which grow slowly and do not affect lifespan.[1] While PSA screening has declined from its peak, most PrCa is still screen-detected and, therefore, likely to be indolent, requiring no treatment. Unfortunately, there is no reliable technology to identify the rare aggressive cancers among the mass of indolent screen-detected PrCa, which has led to frequent overtreatment by surgery or radiation. A lot of effort has been focused on the development of tissue or serum biomarkers to differentiate indolent from aggressive disease, but this has not yet yielded sensitive and specific clinical tools. Consequently, the current clinical paradigm for screen-detected PrCa is active surveillance[2,3] (AS): monitoring by serum PSA testing and serial prostate biopsies to determine the grade (Gleason score) and extent of tumor.

There is an urgent need for imaging tools for AS, (i) to confirm the initial PSA-based diagnosis; (ii) to guide biopsies, which are now performed in a blinded manner; and (iii) to monitor tumor volume, which is currently not measureable but may represent a biomarker of progression from indolent to aggressive disease. Multiparametric magnetic resonance imaging (MRI) may fill some of these roles, but it is expensive and technically limited.[4] In contrast, photoacoustic imaging (PAI), an emerging, noninvasive, functional molecular imaging modality that has not yet entered the clinic, is likely to be less expensive and more portable than any MRI system. The photoacoustic (PA) signal is an ultrasound (US) wave generated by tissue constituents [hemoglobin (Hb), fat, water, and so on] following absorption of short (nanosecond) pulses of laser light in the near-infrared (NIR) spectrum.[5] PAI can discriminate among such tissue constituents on the basis of optical absorption properties, allowing for PAI spectroscopy, which can detect biological function.[6]

Human PrCa is a viable candidate for PAI since transrectal probes can image the prostate gland *in situ*. Based on US data from human PrCa patients, we estimate that the distance from the rectal wall to the anterior prostate is ~3.5 cm (VD, BC, JJK, KLN, unpublished data), which is within the range of depth detection of PAI for PrCa.[7] The most common application of PAI spectroscopy in cancer imaging exploits differences in the absorption spectra of Hb and HbO_2 and is therefore capable of detecting tumors based on regions of hypoxia, that promote neoangiogenesis and more aggressive cancers.[8] However, endogenous tissue constituents, such as Hb, generate relatively weak photoacoustic signals (due to a small absorptivity factor or extinction coefficient) and lack cancer specificity. Exogenous agents, such as NIR-absorbing dyes or gold particles, linked to tumor-specific binding molecules, such as antibodies, can act as targeted molecular imaging agents (TMIAs) to facilitate sensitive and specific detection of the corresponding cancer. Several TMIAs-targeting PrCa have been reported, but while overexpressed in some PrCa, the targets (GRPR and Her2) are more widely expressed.[9] In contrast, PSMA is highly specific and detected on the surface of nearly every human PrCa,

*Address all correspondence to: Kent L. Nastiuk, E-mail: kent.nastiuk@roswellpark.org

†These authors contributed equally to this work.

with low to moderate expression on noncancer prostate tissue and very low expression outside the prostate, making it an excellent biomarker for molecular imaging of PrCa.[10] Unfortunately, the FDA-approved application of PSMA detection (ProstaScint) is of limited value because while PSMA is an excellent target, ProstaScint employs a monoclonal antibody against the internal (cytoplasmic) domain of PSMA, and so detects only necrotic cells.[11] Subsequently, improved PSMA-binding agents have been developed, including a nuclease-stable ribonucleic acid aptamer (A10-3.2) that binds very efficiently.[10] PSMA also has an unusual extracellular active site encoding glutamate carboxypeptidase activity, allowing for the synthesis of a urea-based peptidomimetic inhibitor (DCL), that has been linked to a NIR dye for successful *in vivo* imaging of PSMA+ mouse xenografts[12] and for radiometric imaging of PrCa in patients.[13]

2 Materials and Methods

Figure 1 shows the PAI instrument we employed in this study, similar to the prototype we described previously.[14] Following laser excitation, PA signals from all the absorbers in a small volume of tissue are simultaneously focused on an US detector using an acoustic lens, which corrects for loss of lateral image resolution.[15] The acoustic lens eliminates the need for expensive and time-consuming off-line computer algorithm-based image reconstruction, reducing errors in the final image. This may facilitate more rapid translation to the clinic. Our PA imaging device is comprised of four modules: (i) a fiber-coupled tunable NIR-pulsed laser with wavelengths ranging from 700 to 1000 nm, pulse repetition frequency of 10 Hz, and pulse duration of 5 ns with a surface laser energy intensity of ~20 mJ/cm^2; (ii) an unfocused 32-element (1×0.7 and pitch of 0.7 mm) linear US sensor array with a central frequency of 5 MHz (range 2 to 8 MHz) and 60% bandwidth; (iii) a spherical acoustic lens with a diameter of 25.4 mm and focal length of 39.8 mm to focus PA signal on the sensors; and (iv) a custom designed 32-channel simultaneous data acquisition unit to amplify (40 to 70 decibels variable gain), digitize (12-bit, 30 MHz), average (8×), and store the received PA signals. To acquire C-scan PA planar images, the device is raster-scanned over the cone shaped (20 mm × 1 to 2 mm) sample cuvette using dual-axis stepper motors, while the laser light is delivered using a trans-illumination setup. Previously we used this system to image phantoms[14] and *ex vivo* human PrCa specimens.[16]

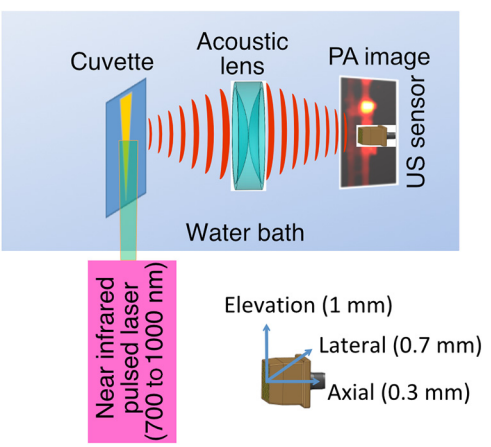

Fig. 1 PAI device configuration. A schematic of the sample cuvette in the instrument and the US 32 sensor linear array-transducer elevation stepped to yield the c-scan image (with oriented resolution).

3 Results

3.1 *Identification of Optimal Chromophore for Imaging Agent*

In order to improve depth penetration and image quality, exogenous chromophores can be employed as contrast agents as part of a TMIA. Using a laser tuned to the maximum excitation wavelength of the TMIA-chromophore, tumor detection can be greatly enhanced as these exogenous chromophores have absorptivity factors two- to three-orders of magnitude greater than those of endogenous agents such as Hb.[15] For greatest tissue depth penetration and sensitivity, TMIAs labeled with chromophores that absorb in the "biological NIR window" between 750 and 900 nm circumvent the natural absorbance of Hb, HbO_2, and H_2O. To identify a suitable NIR dye, optical absorbance of a 100-μM solution of five commercially available dyes IRDye800CW (Licor), Cy7 (synthesized by H.S.), AlexaFluor750, Cyanine7-sulfo, and Dylight800 (ThermoFisher) was first measured to ensure concordance with supplier data after dilution [Fig. 2(a)]. As expected from the reported peak intensities (lambda max), the Alexafluor 750 and Cy7 have a peak optical absorption when irradiated at 750 nm, Cy7-sulfo

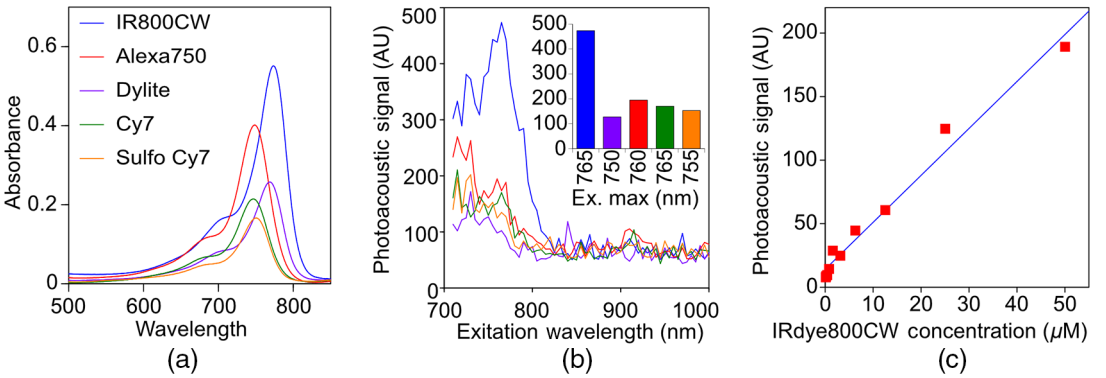

Fig. 2 Optical and photoacoustic spectra of candidate NIR dyes. (a) Optical absorption spectra of indicated NIR dyes. (b) Photoacoustic spectra of the five NIR dyes. Inset: Wavelength (5 nm step indicated below) with the maximal photoacoustic intensity (y-axis, AU: arbitrary units) for the NIR dyes [same color coding for dyes in both graph and inset as in (a)]. (c) Photoacoustic signal intensity at 765 nm correlates with IRdye800CW concentration.

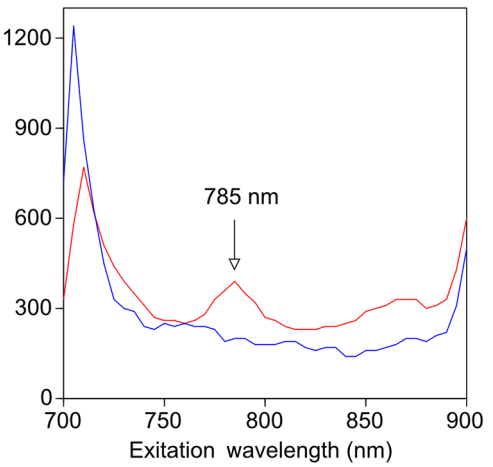

Fig. 3 Specific labeling by TMIA for PAI. PSMA+ C4-2 (red) and PSMA- PC3 (blue) prostate cancer cells were labeled with A10-3.3-IRDye800CW and scanned from 700 to 900 nm wavelength laser light in the instrument shown in Fig. 1.

at 755 nm, Dylight800 at 785 nm, and the dye IR800CW at 775 nm. The spectra of the photoacoustic signal of a 100-μM solution of each contrast agent was then determined over the 710- to 1000-nm wavelength range [Fig. 2(b)]. The inset shows the maxima of each PA signal and the corresponding wavelength (indicated beneath) in the 730 to 875 nm window (signal below 730 nm reflects laser output fluctuation). Among the five contrast agents/dyes we investigated, IRDye800CW was chosen because it produced the highest PA intensity relative to the other agents and because the peak absorption is well separated from endogenous tissue constituents [Fig. 2(b)]. IRdye800CW was serially diluted in DMSO and water. The resultant PA signal intensity above diluent signal correlates well with concentration [$r^2 = 0.979$; Fig. 2(c)]. Using our PAI apparatus with the acoustic lens in-line, 0.8-μM IRDye800CW is the threshold for detecting signal above noise.

3.2 *Photoacoustic Signal from Target Expressing Prostate Cells*

A TMIA was synthesized by labeling the PSMA-specific 10.3.2 aptamer with IRDye800CW (GeneLink). Cells expressing (C4-2) or lacking (PC3) PSMA were incubated in a 4-μM solution of

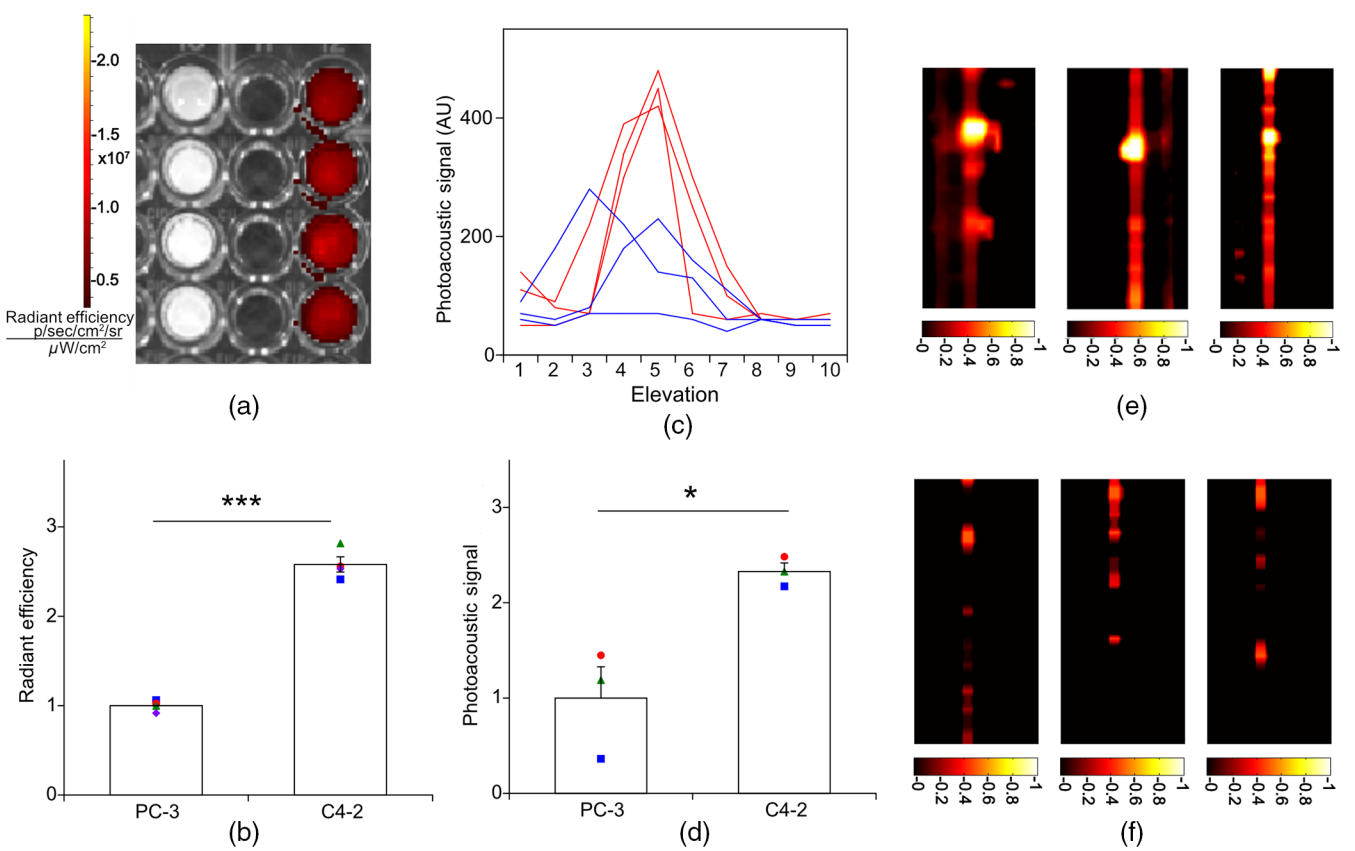

Fig. 4 Enhanced photoacoustic signal from PSMA+ C4-2 PrCa cells labeled with A10-3.2-IRdye800CW aptamer-dye. Optical imaging of a multiwell plate containing aliquots of PSMA+ C4-2 (right side four wells) and PSMA- PC3 (left side four wells) cells labeled with aptamer-dye (buffer in middle wells). Fluorescent signal intensity was captured via (a) IVIS and (b) relative intensity plotted, $p < 0.001$. (c) Cells from three of each of the wells in (a) were sequentially loaded into the PAI instrument cuvette (Fig. 1) and PA signal (B-scan) was captured at 785 nm from c4-2 (red lines) and PC3 (blue lines), by scanning the elevation (long) axis of the cuvette, elevation position (arbitrary) of the probe and (d) peak PA signal was plotted, $p = 0.0174$. C-scan images of cuvettes from (c) containing labeled (e) C4-2 and (f) PC3 cells.

the TMIA in PBS, washed thrice in PBS by centrifugation and resuspension, and examined in our PAI system. The spectra of the photoacoustic signal from C4-2 cells and PC3 cells shows a maximal PA signal difference at 785 nm (Fig. 3). The acoustic lens allows signal detector signal focus from a large incident angle thereby enhancing detection up to fourfold [data not shown (DNS) and Ref. 14]. The 20-nm difference in the wavelength producing peak PA signal between the IRdye800CW alone, at 765 nm, and this 785 nm peak suggests that conjugation of the IRDye800CW to the aptamer to constitute the TMIA, and/or binding of the TMIA to the PSMA molecules on the prostate cell surface, affected the wavelength of absorbance producing the peak PA signal (Fig. 3).

3.3 *Quantitative Assessment of Aptamer as Targeting Agent*

Quantitative characterization of this TMIA shows specific and uniform binding to PSMA-expressing PrCa cells. Four samples of ten million PC3 or C4-2 cells were labeled as above and imaged at 770 nm [Fig. 4(a)] and fluorescence emission was quantitated [Fig. 4(b)] using an IVIS spectrum (Perkin Elmer). TMIA labeling was uniform (CV = 5.5% for PC3, 6.0% for C4-2) and the signal (C4-2) to noise (PC3) ratio (SNR) was 2.56 ± 0.08. One of the four TMIA-labeled cell samples was used to tune the PA system alignment, and the remaining three were sequentially pipetted into the PA cuvette (Fig. 1) and peak PA signal determined at 785 nm excitation from a B-scan [Fig. 4(c)] for each of the six samples. When quantitated, the SNR was 2.33 ± 0.09 [Fig. 4(d)]. The B-scan data were reconstructed as C-scan depicting each cuvette of C4-2 cells [Fig. 4(e)] and PC3 cells [Fig. 4(f)]. Analyzing the C-scan signal using ROIs encompassing each of the six cuvettes, the PA SNR was 5.35 ± 0.04.

3.4 *Quantitative Assessment of Inhibitor as Targeting Agent*

An alternate targeting moiety, consisting of the DCL inhibitor conjugated to IRDye800CW (YC-27, Licor) was similarly evaluated as a TMIA. As above, there was a 20-nm shift in the wavelength of absorbance producing peak PA signal, to 785 nm (DNS). The YC-27 TMIA also shows specific and uniform binding to PSMA-expressing PrCa cells as assessed by fluorescence imaging at 770 nm [Figs. 5(a) and 5(b)]. Variability of YC-27 TMIA labeling was somewhat higher than for the aptamer TMIA (CV = 17% for PC3, 9.9% for C4-2), but the fluorescent SNR was much larger, 24.7 ± 1.22 (versus 2.56 for the aptamer). Peak PA signal from a B-scan for each cell type after labeling with the YC-27 TMIA [Fig. 5(c)] produced an

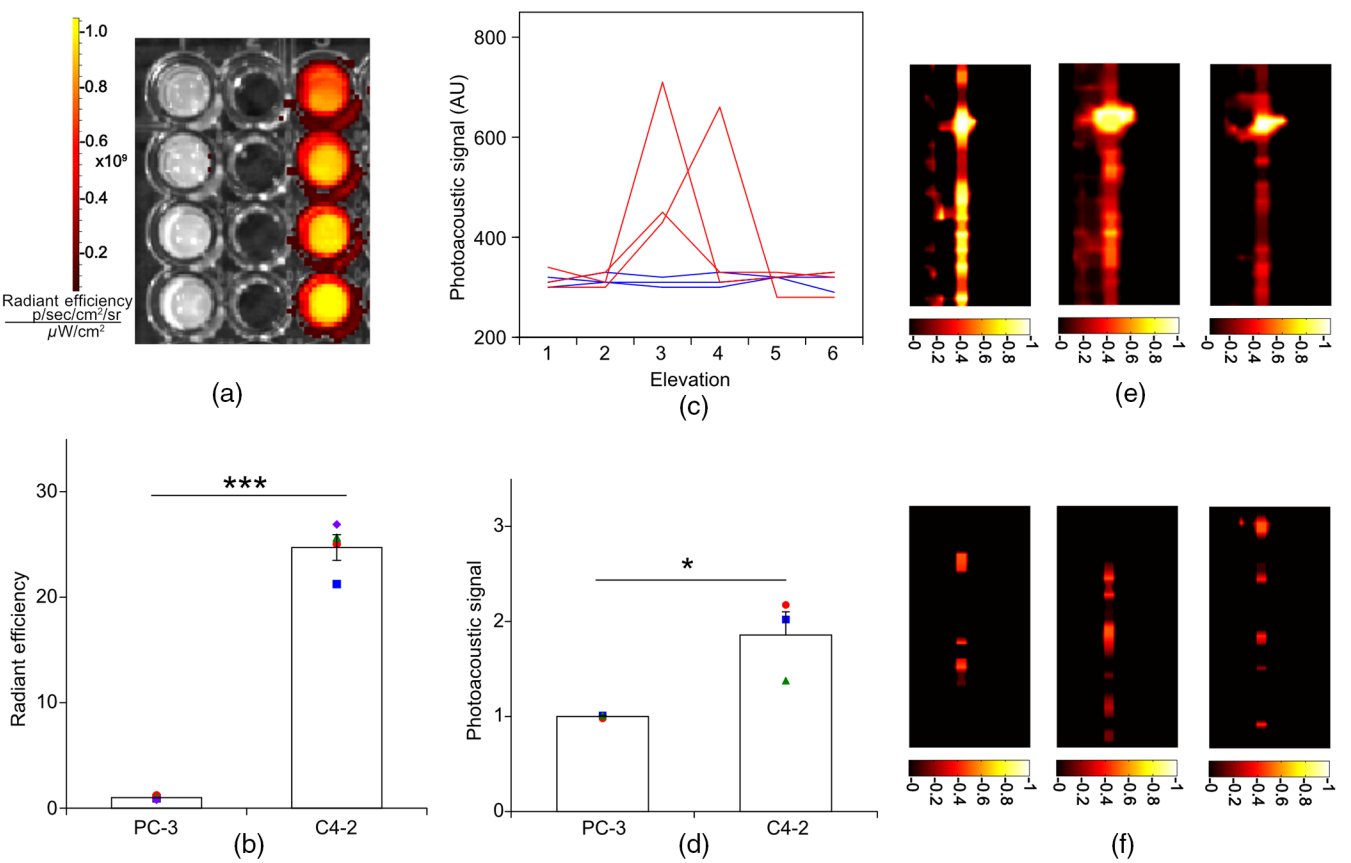

Fig. 5 Enhanced photoacoustic signal from PSMA+ C4-2 PrCa cells labeled with YC27 TMIA. Optical imaging of a multiwell plate containing aliquots of PSMA+ C4-2 (right side four wells) and PSMA- PC3 (left side four wells) cells labeled with urea-dye (buffer in middle wells). Fluorescent signal intensity was captured via (a) IVIS and (b) relative intensity plotted, $p < 0.001$. (c) Cells from three of each of the wells in (a) were sequentially loaded into the PAI instrument cuvette (Fig. 1) and PA signal (B-scan) was captured at 785 nm from c4-2 (red lines) and PC3 (blue lines), by scanning the elevation (long) axis of the cuvette, elevation position (arbitrary) of the probe and (d) peak PA signal was plotted, $p = 0.0246$. C-scan images of cuvettes containing C4-2 (e) and PC3 (f).

SNR of 1.86 ± 0.24 [Fig. 5(d)]. Figures 5(e) and 5(f) are C-scans depicting each cuvette of C4-2 cells and PC3 cells, respectively. Analyzing the C-scans using an ROI encompassing each cuvette, the PA SNR was 5.91 ± 0.81.

4 Discussion

TMIAs optimized for PAI, in combination with an acoustic lens, allowed us to discriminate between PrCa cells lines that either express PSMA or do not express PSMA. Both the A10 aptamer and the DCL inhibitor specifically bind PSMA-expressing cells and are compatible i.p. or intratumoral delivery *in vivo*.[10,17,18] While the aptamer TMIA showed slightly better SNR for PAI, it is expensive to synthesize and less stable than the inhibitor. The YC-27 is much brighter by fluorescence and conjugation of modified chromophores to the DCL inhibitor is more tractable.[18] The urea-targeting agent therefore represents a better approach to developing "louder" TMIAs that will be necessary to overcome the challenges to detecting PrCa by PAI *in vivo*, intensity of light penetration to deep tissue, and TMIA-chromophore abundance due to target density from small tumors.

Acknowledgments

This research was supported by the NIH (R01 CA151753, JJK; R15 CA192148, HS, R15 EB019726, NR, P30CA16056, and P30AR061307), DoD (PC131522, VD), and the SAS (615SF, KLN).

References

1. R. L. Siegel, K. D. Miller, and A. Jemal, "Cancer statistics, 2016," *CA Cancer J. Clin.* **66**, 7–30 (2016).
2. M. L. McDonald and J. K. Parsons, "The case for tailored prostate cancer screening: an NCCN perspective," *J. Natl. Compr. Cancer Network* **13**, 1576–1583 (2015).
3. S. M. Bruinsma et al., "Active surveillance for prostate cancer: a narrative review of clinical guidelines," *Nat. Rev. Urol.* **13**, 151–167 (2016).
4. D. Fehr et al., "Automatic classification of prostate cancer Gleason scores from multiparametric magnetic resonance images," *Proc. Natl. Acad. Sci. U. S. A.* **112**, E6265–E6273 (2015).
5. K. S. Valluru, B. K. Chinni, and N. A. Rao, "Photoacoustic imaging: opening new frontiers in medical imaging," *J. Clin. Imaging Sci.* **1**, 24 (2011).
6. S. Mallidi, G. P. Luke, and S. Emelianov, "Photoacoustic imaging in cancer detection, diagnosis, and treatment guidance," *Trends Biotechnol.* **29**, 213–221 (2011).
7. M. A. Lediju Bell et al., "Transurethral light delivery for prostate photoacoustic imaging," *J. Biomed. Opt.* **20**, 036002 (2015).
8. M. Mehrmohammadi et al., "Photoacoustic imaging for cancer detection and staging," *Curr. Mol. Imaging* **2**, 89–105 (2013).
9. J. Levi, A. Sathirachinda, and S. S. Gambhir, "A high-affinity, high-stability photoacoustic agent for imaging gastrin-releasing peptide receptor in prostate cancer," *Clin. Cancer Res.* **20**, 3721–3729 (2014).
10. J. P. Dassie et al., "Systemic administration of optimized aptamer-siRNA chimeras promotes regression of PSMA-expressing tumors," *Nat. Biotechnol.* **27**, 839–846 (2009).
11. P. M. Smith-Jones et al., "In vitro characterization of radiolabeled monoclonal antibodies specific for the extracellular domain of prostate-specific membrane antigen," *Cancer Res.* **60**, 5237–5243 (2000).
12. Y. Chen et al., "A low molecular weight PSMA-based fluorescent imaging agent for cancer," *Biochem. Biophys. Res. Commun.* **390**, 624–629 (2009).
13. S. P. Rowe et al., "Comparison of prostate-specific membrane antigen-based 18F-DCFBC PET/CT to conventional imaging modalities for detection of hormone-naive and castration-resistant metastatic prostate cancer," *J. Nucl. Med.* **57**, 46–53 (2016).
14. K. S. Valluru et al., "Development of a c-scan photoacoustic imaging probe for prostate cancer detection," *Proc. SPIE* **7968**, 79680C (2011).
15. N. A. Rao et al., "Acoustic lens characterization for ultrasound and photoacoustic C-scan imaging modalities," in *Conf. Proc. IEEE Engineering in Medicine and Biology Society 2008*, pp. 2177–2180 (2008).
16. V. S. Dogra et al., "Multispectral photoacoustic imaging of prostate cancer: preliminary ex-vivo results," *J. Clin. Imaging Sci.* **3**, 41 (2013).
17. X. Ni et al., "Prostate-targeted radiosensitization via aptamer-shRNA chimeras in human tumor xenografts," *J. Clin. Invest.* **121**, 2383–2390 (2011).
18. Y. Chen et al., "Synthesis and biological evaluation of low molecular weight fluorescent imaging agents for the prostate-specific membrane antigen," *Bioconjugate Chem.* **23**, 2377–2385 (2012).